



Synthesis of Hydrogen Getter $Zr_{1-x}Co_x$ ($x=0-1$) Alloy Films by Magnetron Co-Sputtering

Baban P. Dhonge¹, Akash Singh^{1,*}, Arun K. Panda¹, Velaga Srihari², R. Thirumurugesan¹, Pradyumna K. Parida¹, R. Mythili¹ and P. Parameswaran¹

¹Physical Metallurgy Division, Metallurgy and Materials Group, Indira Gandhi Centre for Atomic Research, Kalpakkam 603102, India

²High Pressure and Synchrotron Radiation Physics Division, Bhabha Atomic Research Centre, Mumbai 400085, India

Abstract: The $Zr_{1-x}Co_x$ ($x=0, 0.25, 0.53, 0.63, 1$) thin films were deposited on quartz substrate using magnetron co-sputtering of Zirconium and Cobalt targets in confocal geometry. A constant pulsed direct current (PDC) on Zirconium and radio frequency (RF) of various powers on Cobalt target were applied to vary the concentration of Co in the $Zr_{1-x}Co_x$ film. The film composition was quantified using EDX measurements. The hydrogen storage capacity of these films was studied using an in-house developed hydrogen adsorption setup, in which the electrical resistivity of the film was monitored as a function of hydrogen partial pressure and temperature. The films' surface morphology and crystal structure before and after hydrogenation were characterized using atomic force microscopy and grazing incidence X-ray diffraction techniques using synchrotron radiation, respectively. An increase in the particle size after hydrogenation was observed for all the films. An increase in resistivity was also observed due to the absorption of hydrogen in all the compositions. The near stoichiometric film $Zr_{0.47}Co_{0.53}$ showed the highest hydrogen absorption level at 200 °C at all partial pressures. However, a decrease in the response at temperatures higher than 200 °C was observed in the film containing a Co concentration. The mechanism for the increase in resistivity of the film on hydrogenation is explained.

Received on 22-10-2020
Accepted on 28-12-2020
Published on 31-12-2020

Keywords: ZrCo alloy, hydrogen getter, magnetron co-sputtering, four-probe resistivity, thin film.

DOI: <https://doi.org/10.6000/2369-3355.2020.07.01>

1. INTRODUCTION

It has been discovered that metal hydrides and complex hydrides offer a safe and volume-efficient way to store hydrogen isotopes as compared to the conventional high-pressure cylinders and liquid hydrogen storage methods [1]. Extensive literature is available on the hydrogen storage in bulk materials, while minimal work has been reported on thin films [1-7]. Therefore, the hydrogenation of thin films is an emerging field of research interest. Thin films with nanometric particle size provide a large surface area, leading to fast charging-discharging rates and reduce the absorption/desorption temperature for hydrogen isotopes. The hydrogen molecule dissociates to atomic hydrogen at the surface of the material, and its dissolves in the lattice by penetration surface. However, thin films have a limitation towards the measurement of the P-C-T isotherm due to their capability to absorb a minimal amount of hydrogen compared to that of bulk materials. Also, a protecting layer of active

catalytic material is required to prevent oxidation and contamination from other gases [2]. Hence, monitoring the changes in thin-film resistivity has been adopted as an indirect method to assess the extent of hydrogen absorption by various researchers [2, 5-7]. In general, the surface electrons are mostly contributing to the conduction in a metallic film. The resistance of the film was increased on the absorption of hydrogen molecules due to dissociation to atomic hydrogen by taking an electron from the surface of the film. The four-probe measurement is a well-known method to study the conduction of the thin films. It can measure the very small change in resistance and eliminate the error due to the probe contact.

The development of tritium storage material, which replaces the existing radioactive uranium, is of great interest in Fast Breeder Reactors (FBR) and Thermonuclear Experimental Reactor-Supply and Delivery Systems (ITER-SDS) [8-15]. In FBRs, a cold trap mesh is used to trap hydrogen isotope H , D , and T present in the sodium loop. After a few years of continuous operation, this cold trap mesh is replaced after saturation with hydrogen isotopes. The radioactive tritium ion

*Physical Metallurgy Division, Metallurgy and Materials Group, Indira Gandhi Centre for Atomic Research, Kalpakkam 603102, India; Tel: +91-44-27480500; (Ext.) 22630; Fax: +91-44-27480202; E-mail: akash@igcar.gov.in

present in the mesh has to be deactivated by transferring it to a suitable getter material. Studies on metals and alloys like titanium, zirconium, ZrCo, LaNi₄Mn, La-Ni-Al alloys, etc. have been reported for the storage of tritium [8, 16-19]. Among these, ZrCo alloy has been found to be a more promising material, while others are too stable and require very high temperature for the desorption of tritium at the desired pressure. ZrCo phase has body center cubic crystal (bcc) structure, and on hydrogenation, it transforms into a simple orthorhombic (ZrCoH₃) structure accompanied by a volume expansion of 21.8% [20]. Various chemical and physical techniques have been reported to synthesis metal thin films. Among them, magnetron sputtering is one of the promising techniques for metal thin film deposition. The precise control of the grain size in the nanocomposite films prepared by magnetron sputtering could be achieved by optimizing the process parameters such as substrate temperature, bias voltage, discharge current, and partial pressure of reactive gas. With the recent advancement in power supplies, the pulsed dc magnetron sputtering process has become an attractive production deposition technology [21–23]. Hence effort has been made to synthesis Zr_{1-x}Co_x (x=0-1) film by magnetron co-sputtering for hydrogen getter application. In the present study Zr and Co target were sputtered using PDC and RF power supplies, respectively. The deposition rate of each metal can be controlled using two different power supplies based on the sputtering yield of the individual targets.

The aim of the present study is to (a) synthesize and characterize the Zr_{1-x}Co_x (x=0-1) alloy films using magnetron co-sputtering, (b) optimize the composition of the film to identify the efficient operation temperature range for hydrogen absorption and desorption of hydrogen using in-house developed hydrogen absorption/desorption facility and (c) understand the mechanism for the increase in resistivity of the alloy film on the absorption of hydrogen.

2. EXPERIMENTAL DETAILS

2.1. Film Synthesis

Zr_{1-x}Co_x (x=0, 0.25, 0.53, 0.63, 1) alloy films were synthesized by magnetron co-sputtering system as shown in Figure 1a. Metallic sputtering targets of zirconium (99.5%) and cobalt (99.9%) with 3 inch diameter and 0.125 inch thickness were used. The quartz substrate was placed on the substrate rotator at a concentric distance of 10 cm with reference to both the targets. Prior to deposition, the substrate was ultrasonically cleaned in distilled water and acetone. Sputtering was carried out in an argon (Ar) atmosphere with 3.2×10^{-5} and 3.8×10^{-3} mbar of base pressure and working pressure of the chamber, respectively. A constant argon Ar gas flow rate of 40 standard cubic centimeters per minute (sccm) was maintained during sputtering. The targets were sputter-cleaned for ~ 5 min to remove the oxides and impurities on the target surface before actual deposition. Pulsed direct current (PDC) and radio frequency (RF) power supply were used to sputter Zr and Co targets, respectively. During the deposition of thin films, the PDC power to Zr target was maintained constant at 100 W, while the RF power to Co target was varied from 100 to 200 W, which will hereafter be referred to as Zr₇₅Co₂₅, Zr₄₇Co₅₃, and Zr₃₇Co₆₃, respectively. In addition, pure Zr and Co films were also deposited using 100 watts of PDC power and 150 watts of RF power, respectively. The depositions were carried out for 5-7 minutes. The experimental plan is given in the flow chart, as shown in Figure 1b.

2.2. Hydrogen Absorption/Desorption Study

An in-house facility was developed for studying the hydrogen absorption/desorption characteristics, and the schematic of the setup is shown in Figure 2. In this setup, the four-probe resistivity measurement unit and controlled resistive heater plate are kept inside the vacuum chamber. The chamber was

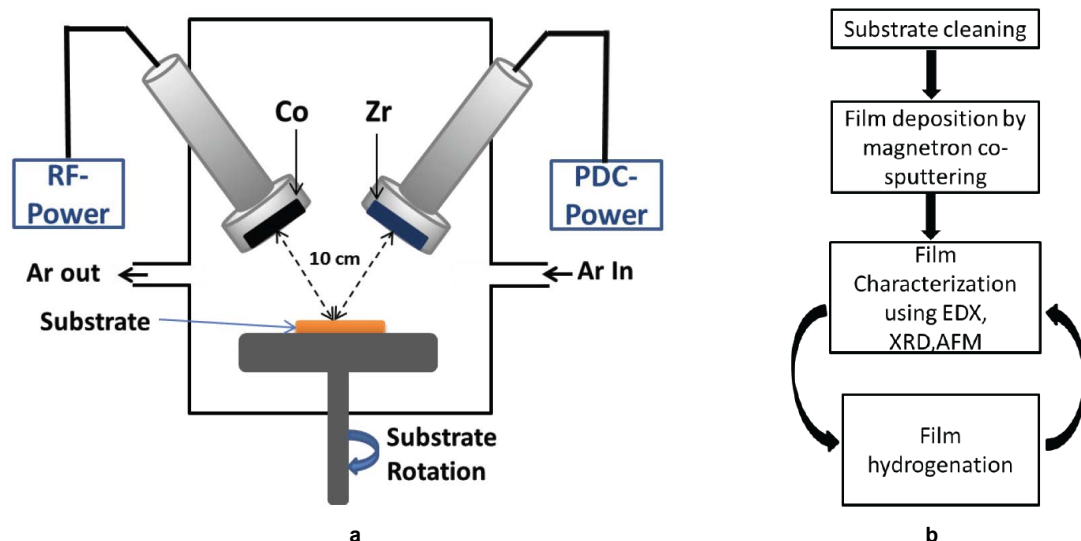


Figure 1: (a): Schematic of magnetron co-sputtering. (b): Flow chart of the experimental plan.

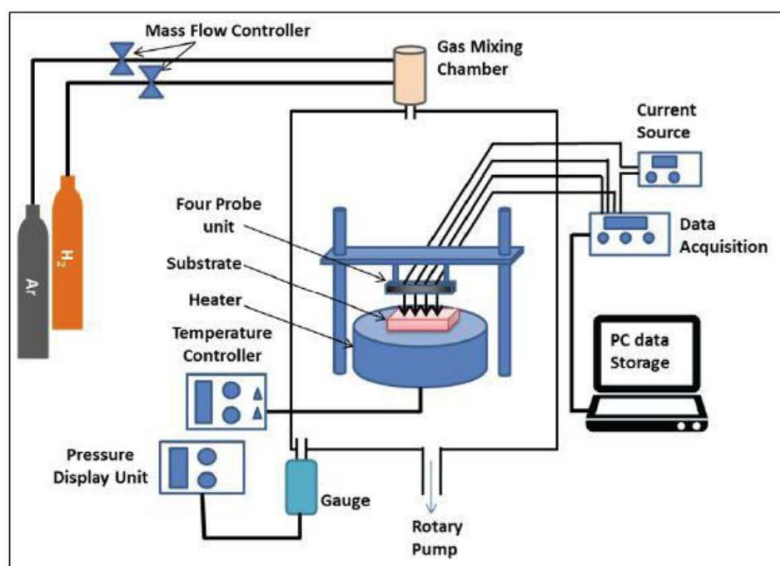


Figure 2: Schematic of the hydrogen absorption setup.

evacuated, and its pressure was monitored using a Pirani gauge (VT Vacuum Techniques LTD, India). Argon and hydrogen gas flow rates were controlled by using a mass flow controller (ALICAT scientific, USA) and mixed before feeding into the chamber. The chamber was flushed with Ar gas 3 times to remove the oxygen and any contamination due to humidity. Further, all the Zr, Co, Zr₇₅Co₂₅, Zr₄₇Co₅₃, and Zr₃₇Co₆₃ films were exposed to various hydrogen partial pressures (H_p) from 0.4 to 1.9 mbar for 10 minutes in the temperature range of 25 to 300°C for three cycles of hydrogen charging. These hydrogen partial pressures were achieved by varying the flow rate of Ar and H₂ gas in 1:1 ratio. The discharge of hydrogen was carried out in Ar atmosphere of 0.4 mbar pressure at the end of each charging cycle. The film's resistance for various partial pressure of hydrogen was recorded using the four-probe resistivity measurement unit. Four spring-loaded electrodes with 2.5 mm inline separation were used to make mechanical contacts on the film surface in the four-probe resistivity measurement unit. Teflon plates with screw fitting hold these electrodes. The coated substrate was kept on the plate heater of diameter 2 inches. A constant current of 0.01 mA was fed across two outermost electrodes using a constant current source (Time Electronic LTD, England), and the corresponding voltage was recorded across the inner two-electrode using Agilent 3497A data acquisition system (Keysight Technologies, USA).

2.3. Characterisation of the Films

After deposition, the thickness of the films was measured using a Dektak surface profilometer. The chemical composition of alloyed films prior to hydrogenation was determined using Energy Dispersive X-ray analysis (EDX) attached to Helios Nanolab 600i dual-beam FESEM. The SE imaging and EDS analysis were carried out at 30keV and 2.7nA beam current. Before and after hydrogenation, the

surface morphology of the films was characterized using atomic force microscopy (AFM, NT-MDT NTEGRA Prima). Synchrotron-based GIXRD measurements on the thin films were carried out using ~ 15 keV x-rays at Extreme Conditions Angle Dispersive/Energy dispersive x-ray diffraction (EC-AD/ED-XRD) beamline (BL-11) at Indus-2 synchrotron source, Raja Ramanna Centre for Advanced Technology (RRCAT), Indore, India. A wavelength of $\lambda \sim 0.80946$ Å was selected for ADXRD diffraction experiments. A MAR345 image plate detector (an area detector) was used to collect 2-dimensional diffraction data. Sample to the detector and the wavelength of the beam was calibrated using NIST standards LaB₆ and CeO₂.

3. RESULTS AND DISCUSSION

3.1. Analysis of Composition and Thickness of Films Prior to Hydrogenation

The Zr_{1-x}Co_x alloyed films' microstructure with an increase in the RF power from 100, 150 to 200 watt and their EDX spectra is shown in Figure 3a-f. Cobalt concentration in the film was found to increase up to 25.3 ± 0.2 , 53.1 ± 0.6 , and 62.8 ± 0.3 atom % with an increase in the RF power from 100, 150 to 200W, respectively. The thickness of Zr, Co, Zr₇₅Co₂₅, Zr₄₇Co₅₃, Zr₃₇Co₆₃, and films were found to be 50 ± 4 , 80 ± 7 , 80 ± 5 , 130 ± 5 , and 150 ± 7 nm, respectively. The thickness of films was found to increase with the increase in the RF power due to the higher sputtering yield of Co as compared to Zr.

3.2. Change in Resistance with Hydrogenation of Zr_{1-x}Co_x Films

The resistance of the Zr_{1-x}Co_x thin films was monitor using the in-housed developed four-probe method. The hydrogen partial pressure (H_p) was step-wise increased at each

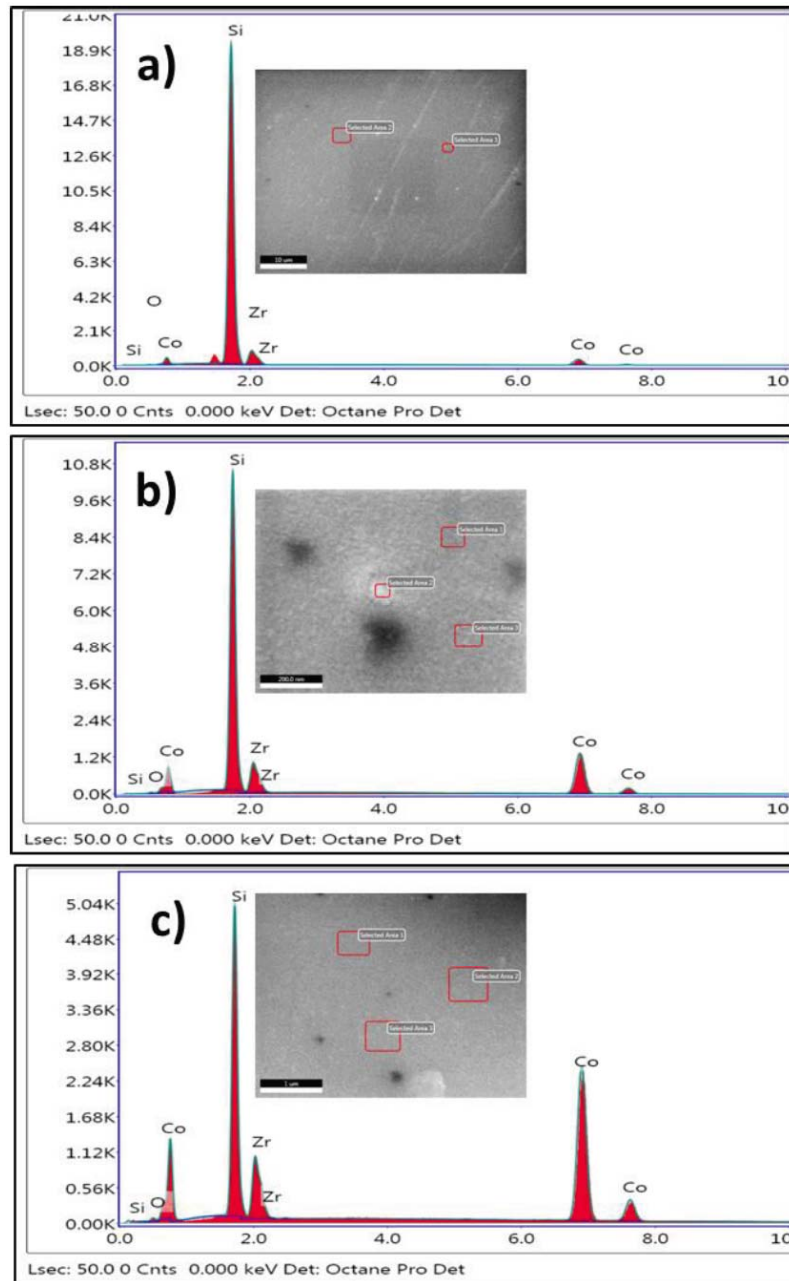


Figure 3: SEM micrographs and EDX spectra of the films deposited using 100 watt PDC (for Zr) and varying RF (for Co) power: (a, b) 100; (c, d) 150 and (e, f) 200 W.

temperature, and the corresponding change in resistance of the films was recorded.

Figure 4 shows the change in resistance of a) Zr, b) $Zr_{75}Co_{25}$, c) $Zr_{47}Co_{53}$, d) $Zr_{37}Co_{63}$, and e) Co films with respect to hydrogen partial pressure in the third hydrogen charging and discharging cycle.

During the first hydrogen charging cycle, a small increase in relative resistance was observed. However, in the second and third cycles, the change in the resistance was found to be almost constant. The first hydrogen cycle activates the film surface by removing the surface contamination like adsorbed oxygen, hydroxide, and carbon oxide molecules [24]. The

resistance of film increases due to the ionization of hydrogen molecule adsorbed on the surface by taking the electron from the film as depicted in eq. 1



The resistance of the films prior to exposure to hydrogen, known as base resistance (R_a), is found to increase with the increase in temperature, thus exhibiting the metallic behavior of the films. Also, the decrease in R_a of the films with an increase in the cobalt concentration is also observed at all temperatures. Hydrogen charging by increasing the hydrogen partial pressure at room temperature does not show any

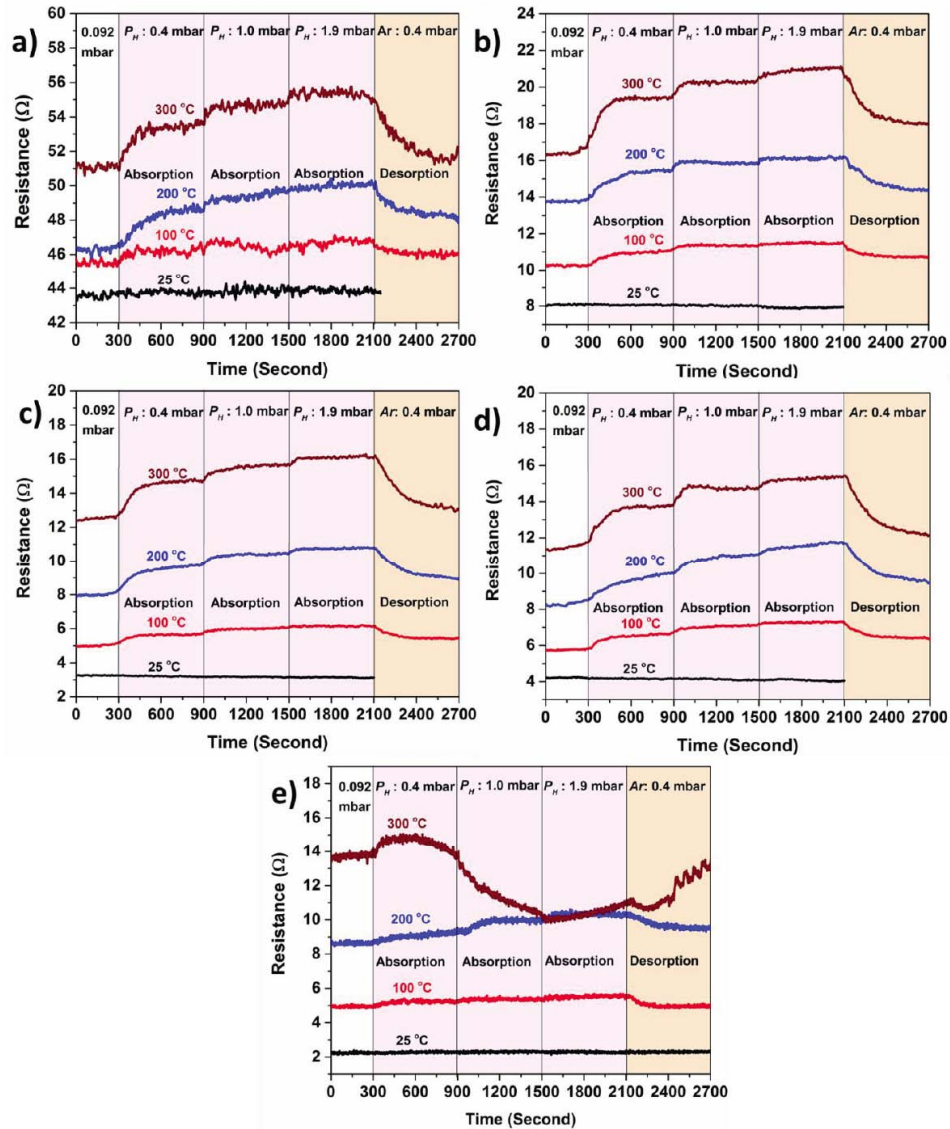


Figure 4: Change in the resistance of the a) Zr, b) $Zr_{75}Co_{25}$, c) $Zr_{47}Co_{53}$, d) $Zr_{37}Co_{63}$, and e) Co films on exposure to the various hydrogen partial pressure (0.4 to 1.9 mbar) for 10 minutes each at different temperature (25 to 300 °C).

change in resistance of all the films, suggesting that no hydrogen absorption took place at room temperature. With the increase in temperature and hydrogen partial pressure, all films show an increase in resistance except for pure Co film at 300 °C. The increase in the resistance of the films on exposure to the hydrogen pressure was found to exhibit kinetics, whose rate is faster initially for a period and then slower, as it is observed that the resistance increases faster during the initial period of 120 to 1180 second and then becomes slower with further increase in time.

Figure 5 shows the relative change in the resistance percentage is also known as response percentage (S) of a) Zr, b) $Zr_{75}Co_{25}$, c) $Zr_{47}Co_{53}$, d) $Zr_{37}Co_{63}$, and e) Co films calculated using the formula

$$S = \frac{R_h - R_a}{R_a} \times 100 \quad (2)$$

Where R_a and R_h are the resistance of the film without (base resistance), and with hydrogen partial pressure, respectively, the response percentage of the Zr and $Zr_{75}Co_{25}$ at various H_p was found to increase with temperature from the RT to 300 °C. The films $Zr_{47}Co_{53}$, $Zr_{37}Co_{63}$, and Co show the first increase in the relative resistance from RT to 200 °C and then decrease at 300 °C. It was observed that the film with the higher Co concentration compared to the stoichiometric ratio of ZrCo alloy showed decreases in S at relatively high temperature, 300 °C. It was also seen that the near stoichiometric film $Zr_{47}Co_{53}$ shows the high response percentage (S) of 18 ± 9 , 30 ± 7 , and 40 ± 7 % for the hydrogen partial pressures of 0.4, 1.0, and 1.9 mbar at 200 °C. Hence, it was concluded that the highest hydrogen absorption occurs for the film of near stoichiometry at 200 °C and up to 1.9 mbar.

As shown in Figure 4c, cobalt film at 300 °C shows the first increase in resistance with H_p during the charging cycle,

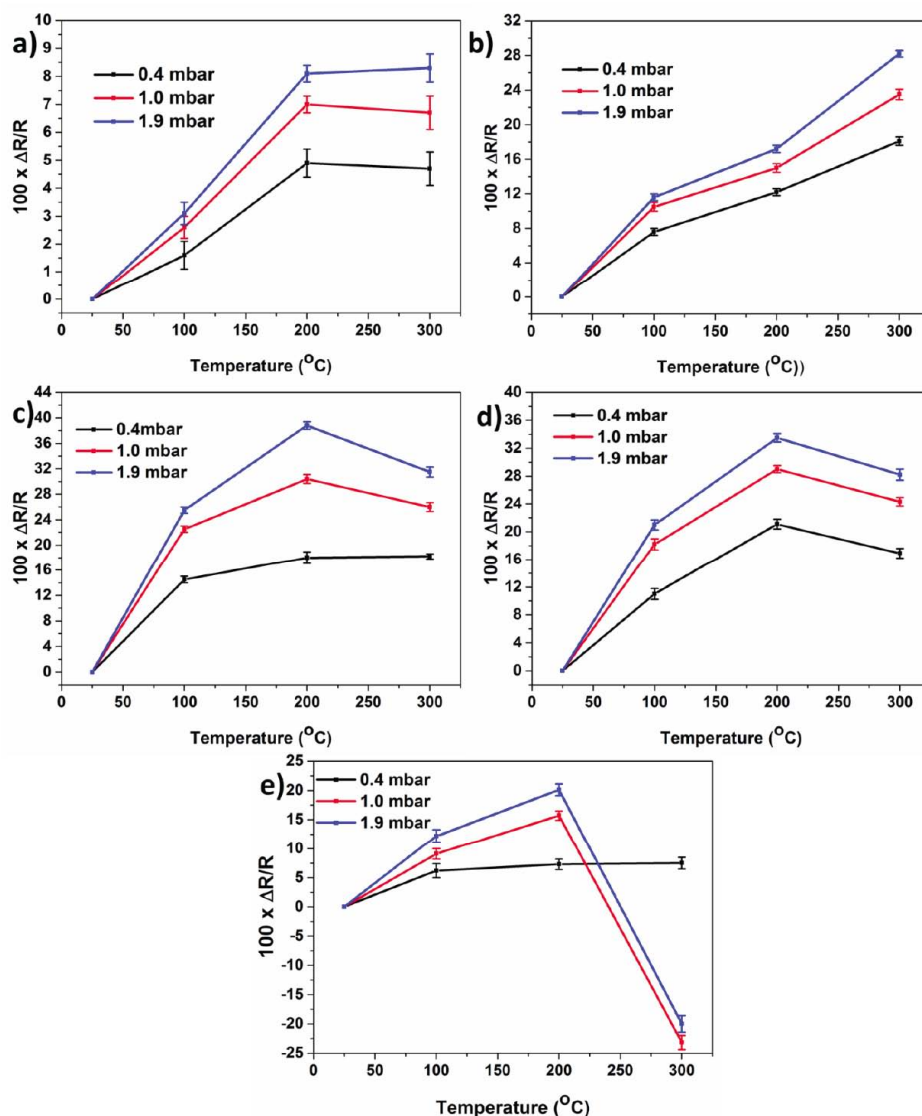


Figure 5: Change in the relative resistance percentage of the a) Zr, b) $\text{Zr}_{75}\text{Co}_{25}$, c) $\text{Zr}_{47}\text{Co}_{53}$, d) $\text{Zr}_{37}\text{Co}_{63}$ and e) Co films on exposure to the various hydrogen partial pressure (0.4 to 1.9 mbar) for 10 minutes each at different temperature (25 to 300 $^{\circ}\text{C}$).

followed by a decrease with further increase in H_p , though during the desorption cycle, an increase in resistance was observed. Also, in Figure 5e, the response percentage showed a drastic decrease at 300 $^{\circ}\text{C}$ at H_p . To understand this behavior, the cobalt film was heated from room temperature to 300 $^{\circ}\text{C}$ at a heating rate of 10 $^{\circ}\text{C}/\text{minute}$, in Ar atmosphere, without and with hydrogen partial pressure of 1 mbar, and corresponding resistance was measured, and the result is shown in Figure 6. The resistance of Co film without P_H is found to increase continuously with temperature, whereas in the presence of hydrogen, the resistance increases from 0.8 to 10 Ω up to a temperature 192 $^{\circ}\text{C}$ and slowly decreases to 8.4 Ω with further increase in the temperature up to 265 $^{\circ}\text{C}$. However, above 265 $^{\circ}\text{C}$ the resistance suddenly dropped to 2.5 Ω at 278 $^{\circ}\text{C}$ and again started increasing with temperature and settled to constant resistance of 8.4 Ω at 300 $^{\circ}\text{C}$. The increase in the resistance is associated with the ionization of hydrogen molecules.

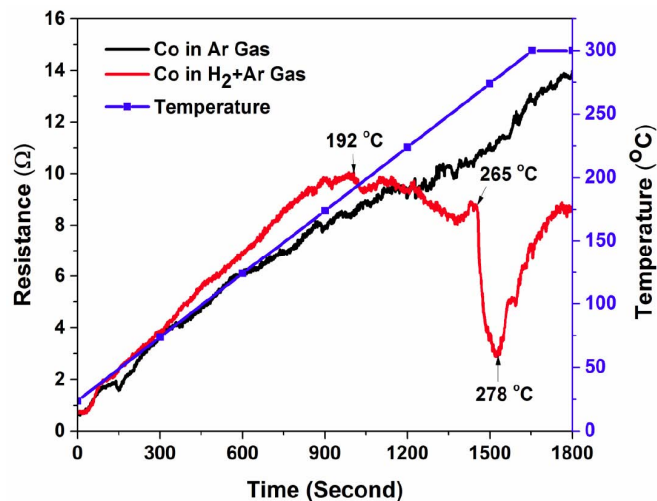


Figure 6: Resistance of Co film with temperature in Ar and H_2+Ar gas pressure.

Table 1: AFMs Grain Size and rms Roughness Analysis of without and with Hydrogenated $Zr_{1-x}Co_x$ alloy Films

$Zr_{1-x}Co_x$ Films	Zr	Zr + H ₂	Zr ₇₅ Co ₂₅	Zr ₇₅ Co ₂₅ + H ₂	Zr ₄₇ Co ₅₃	Zr ₄₇ Co ₅₃ + H ₂	Zr ₃₇ Co ₆₃	Zr ₃₇ Co ₆₃ + H ₂	Co	Co + H ₂
Grain Size (nm)	20 ± 4	25 ± 3	41 ± 6	48 ± 5	26 ± 4	29 ± 5	9 ± 2	13 ± 2	30 ± 2	92 ± 6
Roughness (nm)	3.0	4.4	1.3	2.8	2.2	3.1	2.9	4.0	5.1	10.4

And the decrease in resistance is due to the recombination of these ionized or dissolved hydrogen atoms. The hydrogen desorption from the cobalt surface around 200 °C has been reported by various researchers [25-28]. They found that the desorption temperature varies with the supporting matrix. Recently, it has been reported that the absorption and desorption rates of unsupported cobalt increases with the increase of temperature up to 200 °C and decreases with a further increase in temperature due to the increases in the activation energy hydrogen molecule adsorption [24]. Thus, at the higher temperature, the thermal agitation causes dissolved hydrogen atoms desorption and decreases the absorbed site for hydrogen.

3.3. AFM Studies

The surface morphology of the $Zr_{1-x}Co_x$ alloy film before and after the hydrogenation was characterized using AFM, and the results are shown in Figure 7. The average particle size and surface roughness values evaluated from the analysis of AFM micrographs are tabulated in Table 1. The particle size of as-deposited Zr film was found to increase with the addition of 25% Co ($Zr_{75}Co_{25}$) and decreases with the further addition of Co up to 63% ($Zr_{37}Co_{63}$). Also, an increase in particle size was observed after the hydrogenation of all films was revealed. This might be due to the dissolved hydrogen and effect of hydrogenation at various temperatures [24]. A similar fashion, cobalt film also shows the growth and agglomeration of particles.

3.4. Rationale for Change in Resistance with a Temperature of Hydrogenation

The crystal structure of $Zr_{1-x}Co_x$ alloy films before and after the hydrogenation experiments were characterized using synchrotron radiation GIXRD. Figure 8a-e shows the GIXRD pattern of films before and after the hydrogenation. The presence of a broad peak centered on 11.25° for all the films is due to the glassy structure of the quartz substrate. The peak at 17.08° in Figure 8a for the as-deposited Zr film corresponding to the (002) plane of hcp Zr is found to be shifted to 17.31° after hydrogenation. The alloy films $Zr_{75}Co_{25}$, $Zr_{47}Co_{53}$, $Zr_{37}Co_{63}$ show a broad peak centered at 22.47° and increases in intensity with an increase in Co concentration. The Co film reveals three peaks 21.43°, 22.74°, and 24.11° correspond to (100), (002), and (101) planes of hcp cobalt, respectively. All the hydrogenated films show shifts in the peak positions to the larger 2θ side, due to the stress developed by hydrogen incorporation.

A pictorial representation of hydrogen absorption and desorption mechanism based on the above observations is depicted in Figure 9. Initially, the hydrogen molecules interact with the film and get physically adsorbed on the surface. In the next stage, the physically adsorbed hydrogen molecule gets ionized by taking the electron from the film, forming hydronium ions in the film, which results in a fast increase in resistance during the first 120 to 180 seconds. With further increase in the absorption time at temperatures below 200 °C, these hydronium ions slowly diffuse into the film from the surface, thereby facilitating further adsorption of hydrogen molecules. This causes a slow increase in resistance. However, at temperatures ≥ 300 °C, the thermal agitation does not allow the hydrogen molecule absorption on the film surface and retards the diffusion of hydrogen ion into the film leading to decreases in the resistance. The observed fast drop of resistance of Co film at 265 °C as shown in Figure 6 might be due to the release of diffused hydronium ions. In general, film resistance at a lower temperature is mainly due to the absorption of hydrogen by the film surface by taking an electron. However, at a relatively higher temperature, conduction is due to the hopping of electrons from one grain to another [29].

4. SUMMARY

The Zr-Co alloy films of various compositions Zr, $Zr_{75}Co_{25}$, $Zr_{47}Co_{53}$, $Zr_{37}Co_{63}$, and Co were successfully deposited on the quartz substrate using magnetron sputtering for hydrogen getter application. The hydrogen absorption of these films at various temperatures and hydrogen partial pressures was assessed by measuring resistance using an in-house developed facility. The salient results of the study as follows:

- No hydrogen absorption was observed at room temperature for all films.
- Hydrogen absorption of Zr and $Zr_{75}Co_{25}$ films is found to increase with both temperature and hydrogen partial pressure. $Zr_{47}Co_{53}$, $Zr_{37}Co_{63}$, and Co films exhibited an increase in hydrogen absorption up to 200 °C and decreased at 300 °C for all hydrogen partial pressures.
- The above behavior mechanism is understood to be due to the formation of hydronium ions with an increase in hydrogen partial pressure up to 200°C, beyond which desorption of hydrogen occurs.
- An optimum hydrogen absorption was observed for the near stoichiometric $Zr_{47}Co_{53}$ film up to 200 °C for all partial pressure of hydrogen.

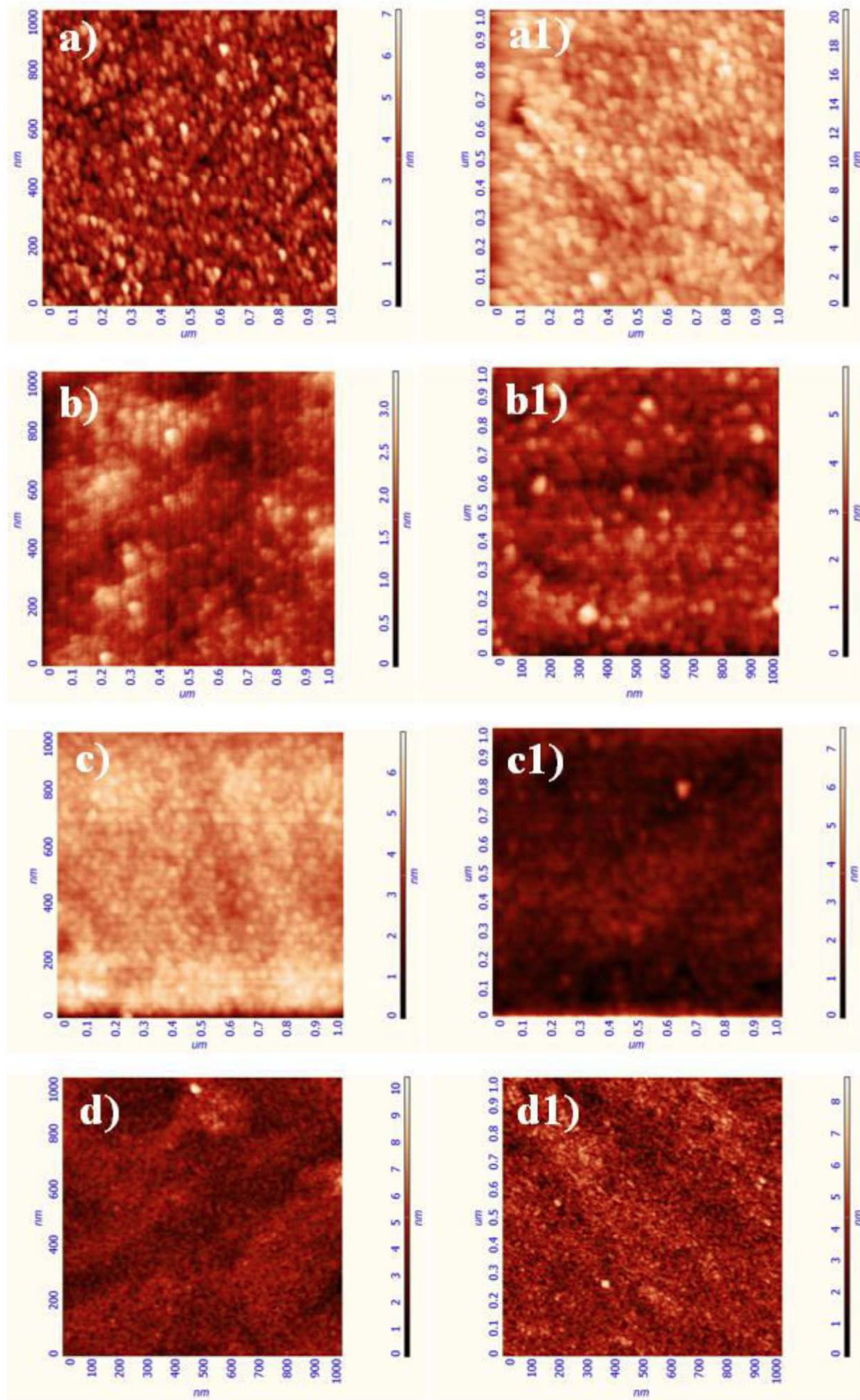


Figure 7: AFM image ($1 \times 1 \mu\text{m}^2$ scanning area) of the film before hydrogenation a) Zr, b) Zr₇₅Co₂₅, c) Zr₄₇Co₅₃, d) Zr₃₇Co₆₃ and after hydrogenation: a1) Zr, b1) Zr₇₅Co₂₅, c1) Zr₄₇Co₅₃, d1) Zr₃₇Co₆₃.

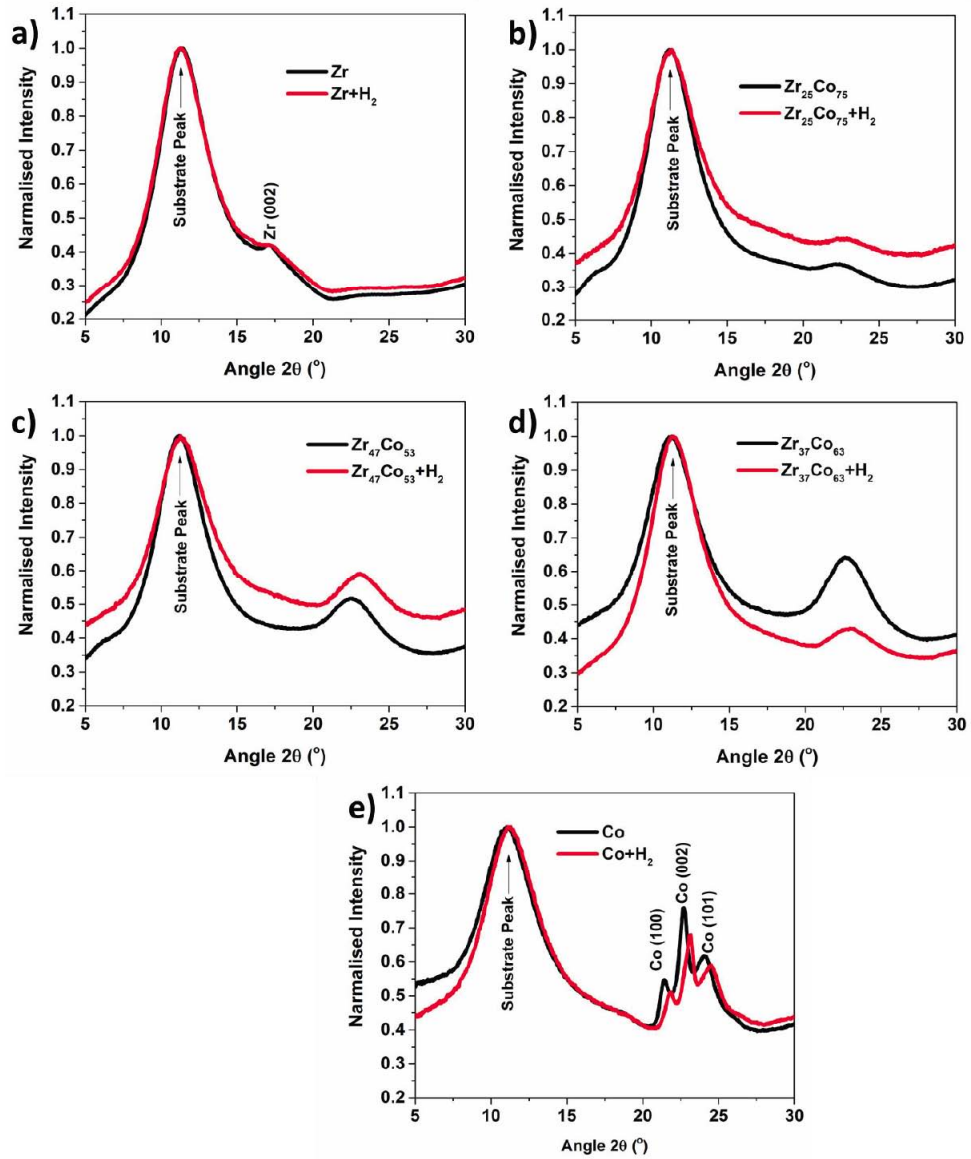


Figure 8: Synchrotron GIXRD pattern of before and after hydrogenated a) Zr, b) Zr₇₅Co₂₅, c) Zr₄₇Co₅₃, d) Zr₃₇Co₆₃, and e) Co films.

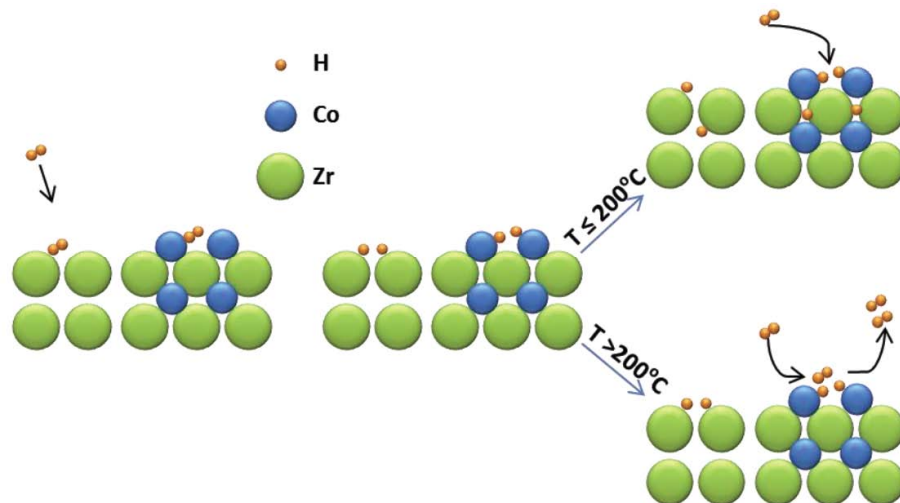


Figure 9: Pictorial representation of the hydrogen absorption and desorption mechanism.

ACKNOWLEDGEMENTS

The authors thank Dr. S. Raju, Associate Director, MCG/MMG/IGCAR and Dr. G. Amarendra, former Director, MMG, IGCAR, Dr. Shaju K Albert, Director, MMG, IGCAR, and Dr. A.K Bhaduri, Director, IGCAR, for their constant encouragement and motivation in the course of the present work. The authors also acknowledge Ms. Jyothi for assisting in the laboratory experiments and the UGC-DAE-CSR Kalpakkam node for providing a microscopy facility.

REFERENCES

- [1] Züttel A. *Materials Today* 2003; 6: 24-33.
[https://doi.org/10.1016/S1369-7021\(03\)00922-2](https://doi.org/10.1016/S1369-7021(03)00922-2)
- [2] Jain IP, Vijay YK, Malhotra LK, Uppadhyay KS. *International Journal of Hydrogen Energy* 1988; 13: 15-23.
[https://doi.org/10.1016/0360-3199\(88\)90005-5](https://doi.org/10.1016/0360-3199(88)90005-5)
- [3] Sakintuna B, Lamari-Darkrim F, Hirscher M. *International Journal of Hydrogen Energy* 2007; 32: 1121-1140.
<https://doi.org/10.1016/j.ijhydene.2006.11.022>
- [4] Chen P, Zhu M. *Materials Today* 2008; 11: 36-43.
[https://doi.org/10.1016/S1369-7021\(08\)70251-7](https://doi.org/10.1016/S1369-7021(08)70251-7)
- [5] Agarwal S, Jain A, Jain P, Vyas D, Ganesan V, Jain IP. *International Journal of Hydrogen Energy* 2010; 35: 9893-9900.
<https://doi.org/10.1016/j.ijhydene.2009.10.003>
- [6] Ingason AS, Olafsson S. *Journal of Alloys and Compounds* 2005; 404-406: 469-472.
<https://doi.org/10.1016/j.jallcom.2005.02.103>
- [7] Singh M, Vijay YK, Jain IP. *International Journal of Hydrogen Energy* 1992; 17: 29-35.
[https://doi.org/10.1016/0360-3199\(92\)90218-L](https://doi.org/10.1016/0360-3199(92)90218-L)
- [8] Penzhorn RD, Devillers M, Sirch M. *Journal of Nuclear Materials* 1990; 170: 217-231.
[https://doi.org/10.1016/0022-3115\(90\)90292-U](https://doi.org/10.1016/0022-3115(90)90292-U)
- [9] Shmayda W, Heics AG, Kherani NP. *Journal of the Less Common Metals* 1990; 162(1): 117-127.
[https://doi.org/10.1016/0022-5088\(90\)90464-U](https://doi.org/10.1016/0022-5088(90)90464-U)
- [10] Cho S, Chang MH, Yun S, Kim DJ. R&D Activities on the Tritium Storage and Delivery System in Korea; 2011.
<https://doi.org/10.13182/FST11-A12602>
- [11] Devillers M, Sirch M, Bredendiek-Kamper S, Penzhorn RD. *Chem Mater* 1990; 2: 255-262.
<https://doi.org/10.1021/cm00009a014>
- [12] Konishi S, Nagasaki T, Okuno K. *Journal of Nuclear Materials* 1995; 223: 294-299.
[https://doi.org/10.1016/0022-3115\(95\)00007-0](https://doi.org/10.1016/0022-3115(95)00007-0)
- [13] Hara M, Okabe T, Mori K, Watanabe K. *Fusion Eng Des* 2000; 49-50: 831-838.
[https://doi.org/10.1016/S0920-3796\(00\)00292-1](https://doi.org/10.1016/S0920-3796(00)00292-1)
- [14] Berkis N, Bessere U, Sirch M, Penzhorn RD. *Fusion Eng Des* 2000; 49-50: 781-789.
[https://doi.org/10.1016/S0920-3796\(00\)00186-1](https://doi.org/10.1016/S0920-3796(00)00186-1)
- [15] Naik Y, Rama Rao GA, Venugopal V. *Intermetallics* 2001; 9: 309-312.
[https://doi.org/10.1016/S0966-9795\(01\)00004-8](https://doi.org/10.1016/S0966-9795(01)00004-8)
- [16] Yaraskavitch JM, Holtslander WJ. Tritium in Metal Hydrides, in: T.N. VeziroĖLu (Ed.) *Metal-Hydrogen Systems*, Pergamon 1982; 619-630.
<https://doi.org/10.1016/B978-0-08-027311-2.50058-9>
- [17] Shanahan KL, Hölder JS, Bell DR, Wermer JR. *Journal of Alloys and Compounds* 2003; 356-357: 382-385.
[https://doi.org/10.1016/S0925-8388\(03\)00139-7](https://doi.org/10.1016/S0925-8388(03)00139-7)
- [18] Moysan I, Contreras S, Demoment J. *Fusion Science and Technology* 2008; 54: 81-84.
<https://doi.org/10.13182/FST08-A1769>
- [19] Cheng GJ, Huang G, Chen M. *Journal of Nuclear Materials* 2018; 499: 490-495.
<https://doi.org/10.1016/j.jnucmat.2017.11.013>
- [20] Chattaraj D, Parida SC, Dash S, Majumder C, *International Journal of Hydrogen Energy* 2012; 37: 18952-18958.
<https://doi.org/10.1016/j.ijhydene.2012.09.108>
- [21] Arnell RD, Kelly PJ, Bradley JW. *Surface and Coating Technology* 2004; 188: 158-163.
<https://doi.org/10.1016/j.surfcoat.2004.08.010>
- [22] Bohlmark J, Christou C, Arutiun P, Ehiasarian, Helmersson U, Alami J. *Journal of Vacuum Science and Technology A* 2005; 23: 18.
<https://doi.org/10.1116/1.1818135>
- [23] Somkhunthot W, Buriinprakhon T, Thomas I, Seetawan T, Amornkitbamrung V. *Elektrika* 2007; 9: 20.
- [24] Bloch J, Brill M, Ben-Eliahu Y, Gavra Z. *Journal of Alloys and Compounds* 1998; 267: 158-166.
[https://doi.org/10.1016/S0925-8388\(97\)00557-4](https://doi.org/10.1016/S0925-8388(97)00557-4)
- [25] Zowtiak JM, Bartholomew CH. *Journal of Catalysis* 1983; 83: 107-120.
[https://doi.org/10.1016/0021-9517\(83\)90034-9](https://doi.org/10.1016/0021-9517(83)90034-9)
- [26] Cabrera AL. *Journal of Vacuum Science and Technology A* 1993; 11: 205-208.
<https://doi.org/10.1116/1.578704>
- [27] Romero CP, Avila JI, Cisternas E, Cabrera GB, Cabrera AL, Temst K, Van Bael MJ. *Journal of Materials Science* 2007; 42: 7667-7672.
<https://doi.org/10.1007/s10853-007-1667-x>
- [28] Spasojevic M, Krstajic N, Zelenovic LR, Maricic A, *Journal of Alloys and Compounds* 2010; 505: 549-554.
<https://doi.org/10.1016/j.jallcom.2010.06.070>
- [29] Neugebauer CA. In: Has George, Thum RE, editors. *Physics of thin films*. New York: Academic Press; 1964: vol. 2: 22-30.